folia medica

Folia Medica 67(2)
DOI: 10.3897/folmed.67.e143604

Original Article

Investigations on the dysregulated genes in high-fat-fed mice infected with *Prevotella intermedia* and their possible role in the development of hepatocellular carcinoma

Yathin Reddy Putta[1], Anitha Pandi[1], Jayaseelan Vijayashree Priyadharsini[1]

1 *Clinical Genetics Lab, Centre for Cellular and Molecular Research, Saveetha Dental College and Hospital, Saveetha Institute of Medical and Technical Sciences, Saveetha University, Chennai, India Saveetha Dental College and Hospitals, Chennai, India*

Corresponding author: Jayaseelan Vijayashree Priyadharsini, Clinical Genetics Lab, Centre for Cellular and Molecular Research, Saveetha Dental College and Hospital, Saveetha Institute of Medical and Technical Sciences, Saveetha University, Poonamalle High Road, Chennai-77, India: Email: viji26priya@gmail.com

Received: 5 December 2024 ♦ **Accepted:** 11 March 2025 ♦ **Published:** 4 April 2025

Citation: Putta YR, Pandi A, Priyadharsini JV. Investigations on the dysregulated genes in high-fat-fed mice infected with *Prevotella intermedia* and their possible role in the development of hepatocellular carcinoma. Folia Med (Plovdiv) 2025;67(2):e143604. doi: 10.3897/folmed.67.e143604.

Abstract

Introduction: Hepatocellular carcinoma (HCC) is a leading global cancer, often linked to various factors, including viral infections and metabolic disorders. Recent studies suggest that microbial infections, particularly from oral pathogens like *Prevotella intermedia* (*Pi*), may elevate the progression of HCC through dysbiosis and chronic inflammation.

Aim: In view of this, the study aimed to identify candidate genes in high-fat diet-fed mice infected with *Pi* and to assess the relevance of these orthologous genes in the development of human HCC.

Materials and methods: The GEO dataset, GSE136937, was employed to identify the differentially expressed genes across two datasets *viz.,* regular chow-fed and high-fat diet-fed mice infected with *Pi.* A comparison was made between normal vs. high-fat diet-fed mice infected with *Pi* to demonstrate the influence of the microbial factor on the development of metabolic disorders and cancer. The identified DEGs were subjected to protein-protein interaction (PPI) analysis and gene ontology (GO) assessments. Human orthologs were evaluated for gene expression status and survival using the TCGA dataset.

Results: The analysis revealed numerous DEGs between infected and uninfected groups. The top 20 DEGs (16 upregulated, 4 downregulated) were further investigated in liver hepatocellular carcinoma patients (TCGA). Notably, genes *RMND1* and *CYP3A43* displayed similar expression patterns in both mouse and human datasets. High *RMND1* expression was associated with poor prognosis, while low *CYP3A43* expression indicated a poor survival outcome in HCC patients.

Conclusion: Metabolic disorders in conjunction with microbial dysbiosis together could support the malignant phenotype by modifying the expression profiles of key genes involved in carcinogenesis. More intense experimental and in vivo studies are needed to further confirm the association of these candidate genes with HCC.

Keywords

gene expression, inflammation, prognosis, survival

Introduction

Hepatocellular carcinoma (HCC) is one of the most common forms of cancer and is reported to be the third leading cause of death globally. HCC constitutes around 80% of all liver cancers across the world. Hepatitis B and C viruses, non-alcoholic fatty liver disease (NAFLD), metabolic disorders, exposure to aflatoxins, environmental factors, and habits such as smoking and alcoholism contribute immensely to the development of HCC.[1] Apart from the known etiology of hepatitis B and C viruses, NAFLD is a significant risk factor for developing HCC. NAFLD is characterized by the accumulation of triglycerides and the activation of the inflammatory process by proinflammatory cytokines. In addition, oxidative stress and mitochondrial dysfunction may contribute to the genetic instability of the hepatocytes.[2] Studies on the effects of microbial infection on the activation of hepatic stellate cells (HSCs), initiation, and progression of hepatocellular carcinoma revealed microbial dysbiosis in patients with liver cancer. The pathogens were found to induce the expression of senescence-associated secretory phenotype (SASP) factors by HSCs, which resulted in carcinogenesis.[3] Another mechanism has been reviewed, which involved the activation of HSCs that form an essential source of cancer-associated fibroblasts in the tumor microenvironment established in the liver. The crosstalk between these cells and the immune cells was known to evade the immune surveillance mechanisms modulated by T regulatory cells and M2 macrophages.[4] Accumulating experimental reports have provided substantial evidence of viruses as potent activators of hepatic stellate cells.[5,6]

The human microbiome comprises all microbes and their genes in the human body. Among all other regions, the gut and oral microbiota play a vital role in metabolism and immune function. Derangements in this microbiome have been associated with chronic liver disease, carcinoma of the head and neck region[7], NAFLD[8], hepatocellular carcinoma, and many more. Even though viruses play a critical role in regulating the transformation of cells, in recent days, researchers have identified bacterial pathogens to be associated with the process of tumor development. One of the pathogens is *Prevotella intermedia (Pi),* a known periodontal pathogen that is Gram-negative and anaerobic. Current research has suggested that *Pi* is strongly associated with several diseases, including cancer. To exert its effect, *Pi* binds to host cells such as gingival fibroblasts via adhesins and cysteine proteases. Co-infection of *Pi* with other microbial pathogens triggers a sustained inflammatory response, inevitably leading to tissue damage and cell transformation.[9] Another study by Qin and colleagues revealed that infection with *Pi* leads to aggressiveness of OSCC, achieved by overexpression of ISG15.[10] Computational approaches have eased identifying differentially expressed genes in various diseases. These genes can be used as potential targets for early detection of pathogen-mediated disease, as therapeutic or prognostic targets.[11] In line with these facts, the present study aimed to assess the synergistic effect exerted by metabolic dysfunction and infection by pathogens on the development of cancer using computational approaches. High-fat-fed mice are more prone to metabolic disorders such as type 2 diabetes mellitus, obesity, cardiovascular diseases, and many more. The rationale behind selecting these high-fat-fed mice for the present study was to demonstrate how microbial dysbiosis, in addition to metabolic dysregulations, paves the way for the development of cancer.

Aim

The study has been designed to identify the differentially expressed genes (DEGs) in high-fat, diet-fed mice treated with *Pi* compared to uninfected, normal, diet-fed mice. The results would provide insight into those genes exclusively expressed in mice with metabolic disorder infected with the oral-dental pathogen, *Pi*. Here, the crosstalk between the genes involved in metabolic disruption and microbial dysbiosis will be analyzed. The DEGs identified were further investigated to demonstrate their expression profiles in liver hepatocellular carcinoma patients (LIHC) to bring in a possible association between the genes expressed in the presence of the microbial pathogen and their human orthologs in connection with the disease.

Materials and methods

Sample dataset

The GEOmnibus dataset GSE136937, consisting of mouse model C57BL/6N/Jcl, was used for the study. The sample dataset taken for the present analysis consisted of 3 samples of regular chow-fed mice (GSM4062010, GSM4062011, GSM4062012), four samples from high-fat-fed mice exposed to *Prevotella intermedia* (GSM4062017, GSM4062018, GSM4062019, GSM4062020) and four samples from untreated high-fat-fed mice (GSM4062013, GSM4062014, GSM4062015, GSM4062016). Gene expression was compared between regular chow-fed mice and the high-fat-fed mice exposed to *Prevotella intermedia.*[8] The adjusted p-value was derived using the Benjamini and Hochberg's method. An adjusted p-value lower than 0.05 was considered significant. The threshold for log 2-fold change was set at 0 and excluded pseudogenes and non-coding RNAs from further analysis. The protocol was reviewed by the Institution Review Board (SRB/SDC/UG-2234/24/MICRO/319), and approval for the same was provided (IHEC/SDC/DT/UG-2234/24/MICRO/227).

Protein-protein interaction (PPI) analysis

A set of the top 20 DEGs (differentially expressed genes) identified in the high-fat diet-fed mice exposed to *Prevotel-*

la intermedia was evaluated for protein-protein interactions of these genes using the STRING (Search Tool for the Retrieval of Interacting Genes/Proteins), version 12. The interaction source included text mining, experiments, databases, co-expression, neighborhood, gene fusion, and co-occurrence sources, with a minimum score of 0.400. The PPI enrichment score evaluates the query protein's observed interactions against the entire proteome. A *p*-value less than 0.05 implies that the observed interactions are statistically significant. This bioinformatics platform provided data on direct physical interactions and functional associations of proteins. In the network, proteins are denoted as nodes, while the edges indicate the type of interaction, whether physical, enzymatic, or genetic.[12]

Gene ontology analysis

The PANTHER database (v16.0; Protein Analysis Through Evolutionary Relationships) was employed for the gene ontology analysis of the curated DEGs in *Mus musculus*. This analysis allowed us to understand the molecular pathways, functions, biological processes, and subcellular localization of gene products. A user-defined query of the top 20 genes was used to identify the pathways in which the genes are clustered. Additionally, we performed pathway-based classification to identify and explore potential pathways associated with the genes, contributing to a more comprehensive analysis.[13,14]

Gene enrichment analysis

Understanding large-scale studies involves identifying crucial biological pathways and protein complexes within intricate datasets. Metascape is a user-friendly web portal that helps experimental biologists analyze and interpret this data type by integrating diverse biological databases and analytical tools. It simplifies the process and provides precise results with features like functional enrichment, interactome analysis, and gene annotation, making it easier for researchers to compare data from different experiments. The present study utilized DisGENET analysis to integrate various data types. The DEGs identified were submitted as a query and checked with the *Homo sapiens*. This process was conducted to analyze the functional role of orthologous genes.[15]

Gene expression and survival analysis

The study analyzed the top 20 DEGs in high-fat-fed mice exposed to *Prevotella intermedia* in the hepatocellular carcinoma dataset using the UALCAN database (http://ualcan.path.uab.edu/cgi-bin/TCGA-survival). The study involved 371 samples from patients with liver hepatocellular primary tumors and 50 paired normal samples. The expression profile was measured in transcripts per million (TPM), a standard unit for normalizing RNA-seq data. The significance between different groups was determined by creating Box-Whisker plots using the TPM values. Additionally, the study demonstrated the overall survival of patients with liver hepatocellular carcinoma (LHCC) using Kaplan-Meier analysis. By comparing the high-expression and low/medium-expression groups, the study illustrated the effect of gene expression changes on patients' overall survival.[16] The Kaplan Meier Survival Plotter was further used to confirm the survival status of LHCC patients upon changes in the gene expression profile of the selected gene (https://kmplot.com/analysis/).[17]

Statistical analysis

The gene expression data from multiple datasets were rigorously analyzed using the powerful GEO2R tool, which effectively leverages R packages from Limma to meticulously examine the microarray data and present results in comprehensive tables and graphic plots.[18] The UALCAN portal conducted a robust analysis of gene expression profiles by comparing expression levels between groups using a PERL script accompanied by the Comprehensive Perl Archive Network (CPAN) module. Additionally, survival plots were generated using the "survival" and "survminer" R packages and compared using the log-rank test. The "survival" package was exclusively utilized to perform thorough survival analysis, including survival curves, hypothesis tests, and models, while "survminer" significantly enhanced the visualization of Kaplan-Meier and forest plots, ensuring a clear and comprehensive representation and interpretation of complex survival data.[19]

Results

DEG analysis and curation of gene dataset

The comparison between high-fat treated mice infected with *Pi* and high-fat-fed mice returned no significant hub of differentially expressed genes **(Fig. 1a)**. Interestingly, the comparison between high-fat-fed obese mice infected with *Pi* and normal diet-fed mice showed a marked difference in the expression of genes **(Fig. 1b)**. Since the collection of genes was exhaustive, the top 20 genes were curated for further analysis. Among the 20 DEGs, 16 were upregulated, and four were downregulated **(Table 1)**. Subsequently, the expression profile of orthologous DEGs identified in mice was assessed in LIHC patients of the TCGA dataset **(Table 2)**.

Protein-protein interaction (PPI) and gene ontology analysis

The protein-protein interaction network of 19 DEGs presented two clusters of proteins: Zbp1, Irf7, Usp18, Abhd2, Ifit3b, and Slc25a27, Cyp3a11, and Cyp3a16. The other proteins remained as independent entities. There were 19 nodes and 7 edges, with a PPI enrichment value of

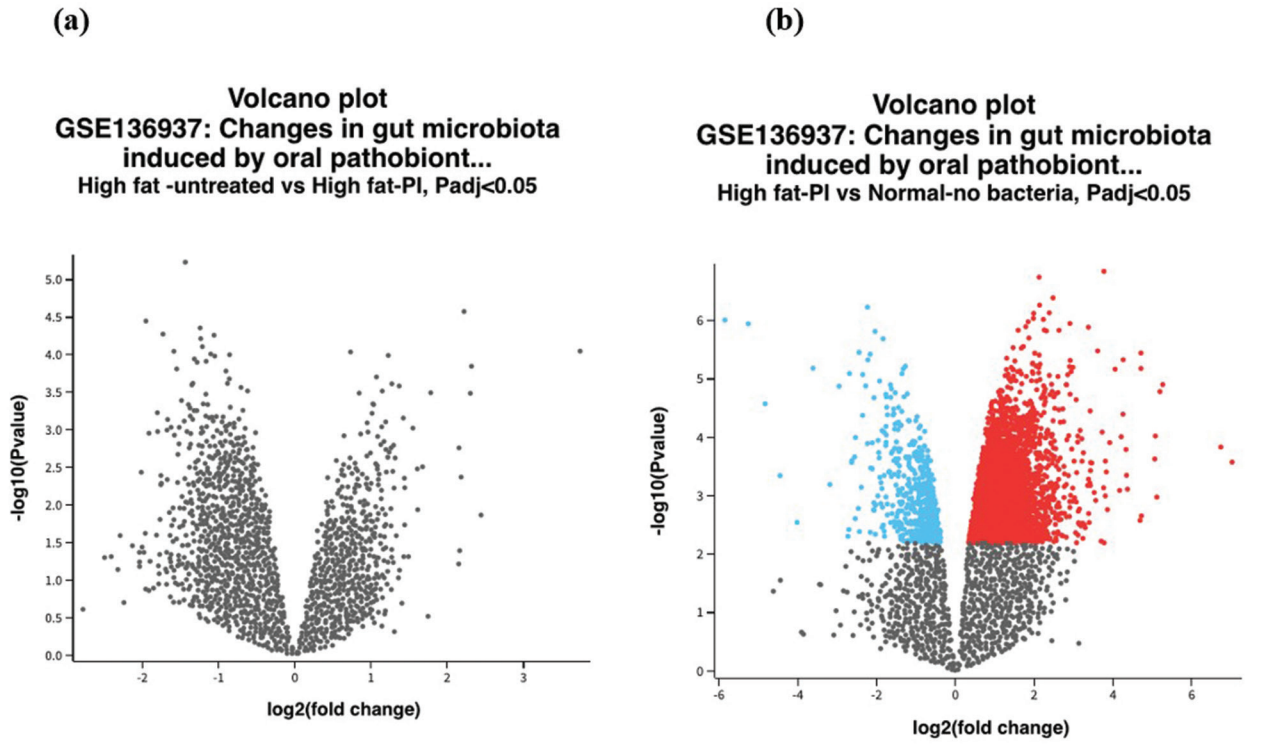

Figure 1. (**a**) Volcano plot demonstrating differentially expressed genes (DEGs) in the liver of high-fat diet-fed C57BL/6 mice treated with *Prevotella intermedia* vs high-fat diet-fed C57BL/6 mice; (**b**) Volcano plot demonstrating differentially expressed genes (DEGs) in the liver of high-fat diet-fed C57BL/6 mice treated with *Prevotella intermedia* vs Untreated C57BL/6 mice. Blue dots indicate genes that are downregulated, and red dots represent genes that are upregulated. A *p*-value less than 0.05 was considered significant.

Table 1. List of top 20 genes differentially expressed in the liver of high-fat diet-fed C57BL/6 mice treated with *Prevotella intermedia* compared to regular chow-fed mice. An adjusted *p*-value of less than 0.05 was considered to be significant

Gene	Protein encoded	Adjusted *p* value	Log Fold Change	Gene expression
GM36283	Predicted gene, 36283	0.00436	3.77	Upregulated
USP18	Ubiquitin specific peptidase 18	0.00436	2.12	Upregulated
SLC26A10	Solute carrier family 26, member 10	0.00436	2.47	Upregulated
SLC25A27	Solute carrier family 25, member 27	0.00436	2.13	Upregulated
CYP3A11	Cytochrome P450, family 3, subfamily a, polypeptide 11	0.00436	−2.23	Downregulated
AMDHD2	Amidohydrolase domain containing 2	0.00436	2.38	Upregulated
RMND1	Required for meiotic nuclear division 1 homolog (*S. cerevisiae*)	0.00436	1.98	Upregulated
SCD1	Stearoyl-Coenzyme A desaturase 1	0.00436	−5.85	Downregulated
MAT2A	Methionine adenosyltransferase II, alpha	0.00436	1.84	Upregulated
DACT1	Dapper homolog 1, antagonist of beta-catenin (xenopus)	0.00436	2.90	Upregulated
ABHD2	Abhydrolase domain containing 2	0.00436	3.37	Upregulated
ZBP1	Z-DNA binding protein 1	0.00436	2.25	Upregulated
MBD4	Methyl-CpG binding domain protein 4	0.00436	1.59	Upregulated
CCND1	Cyclin D1	0.00436	2.63	Upregulated
CYP3A16	Cytochrome P450, family 3, subfamily a, polypeptide 16	0.00436	−2.04	Downregulated
IRF7	Interferon regulatory factor 7	0.00529	1.86	Upregulated
CYP3A59	Cytochrome P450, family 3, subfamily a, polypeptide 59	0.00529	−1.83	Downregulated
HAP1	Huntingtin-associated protein 1	0.00673	1.46	Upregulated
IFIT3B	Interferon-induced protein with tetratricopeptide repeats 3B	0.00673	1.67	Upregulated
CIART	Circadian associated repressor of transcription	0.00707	3.61	Upregulated

Table 2. Gene expression profile and survival analysis of DEGs identified in the high-fat diet-fed C57BL/6 mice treated with *Prevotella intermedia* in liver hepatocellular carcinoma patients. * Non-coding RNAs are excluded from the study

Gene	Protein encoded	Gene expression in mouse liver cells	Gene expression in LIHC	P value	Survival (p value)	Survival outcome
GM36283	Predicted gene, 36283	Upregulated	Data unavailable			
USP18	Ubiquitin specific peptidase 18	Upregulated	Insignificant	2.86×10^{-01}	0.027	High expression, Poor prognosis
SLC26A10	Solute carrier family 26, member 10	Upregulated	Upregulated	1.72×10^{-12}	0.11	Insignificant
SLC25A27	Solute carrier family 25, member 27	Upregulated	Upregulated	7.46×10^{-09}	0.24	Insignificant
CYP3A11/CYP3A5	Cytochrome P450, family 3, subfamily a, polypeptide 11	Downregulated	Insignificant	1.31×10^{-06}	0.36	Insignificant
AMDHD2	Amidohydrolase domain containing 2	Upregulated	Upregulated	1.62×10^{-12}	0.062	Insignificant
RMND1	**Required for meiotic nuclear division 1 homolog (S. cerevisiae)**	**Upregulated**	**Upregulated**	**1.55×10^{-11}**	**0.024**	**Poor prognosis**
SCD1/SCD	Stearoyl-Coenzyme A desaturase 1	Downregulated	Upregulated	1.23×10^{-06}	0.97	Insignificant
MAT2A	Methionine adenosyltransferase II, alpha	Upregulated	Upregulated	2.19×10^{-12}	0.36	Insignificant
DACT1	Dapper homolog 1, antagonist of beta-catenin (xenopus)	Upregulated	Insignificant	6.19×10^{-01}	0.32	Insignificant
ABHD2	Abhydrolase domain containing 2	Upregulated	Downregulated	1.00×10^{-02}	0.93	Insignificant
ZBP1	Z-DNA binding protein 1	Upregulated	Upregulated	3.09×10^{-01}	0.54	Insignificant
MBD4	Methyl-CpG binding domain protein 4	Upregulated	Upregulated	1.99×10^{-11}	0.8	Insignificant
CCND1	Cyclin D1	Upregulated	Downregulated	1.79×10^{-01}	0.95	Insignificant
CYP3A16/CYP3A5	Cytochrome P450, family 3, subfamily a, polypeptide 16	Downregulated	Insignificant	7.94×10^{-01}	0.0077	Poor prognosis
IRF7	Interferon regulatory factor 7	Upregulated	Insignificant	1.41×10^{-01}	0.079	Insignificant
CYP3A59/CYP3A43	**Cytochrome P450, family 3, subfamily a, polypeptide 59**	**Downregulated**	**Downregulated**	**3.98×10^{-07}**	**0.028**	**Poor prognosis**
HAP1	Huntingtin-associated protein 1	Upregulated	Insignificant	1.00×10^{-01}	0.6	Insignificant
IFIT3B/IFIT3	Interferon-induced protein with tetratricopeptide repeats 3B	Upregulated	Insignificant	6.19×10^{-01}	0.99	Insignificant
CIART/C1ORF51	Circadian associated repressor of transcription	Upregulated	Upregulated	1.62×10^{-12}	0.1	Insignificant

Data in bold represent high statistical significance

0.000618 **(Fig. 2)**. The gene ontology analysis using Panther demonstrated the genes related to the following pathways: cell cycle, Huntington's disease, PI3 kinase, S-adenosylmethionine, Wnt signaling, Toll-like receptor, and CCKR signaling pathway **(Fig. 3)**.

Gene enrichment analysis

The gene enrichment analysis performed using Metascape on human orthologs of the mouse DEGs identified returned four significant pathways involved in (**a**) regulation of type 1 interferon-mediated signaling pathway, nuclear receptor meta pathway, DNA damage response pathway, and cellular catabolic pathway. The -log10 p value was highly significant for the interferon-mediated signaling pathway while moderately significant for the cellular catabolic process **(Fig. 4)**.

Gene expression and survival analysis

Among the top 20 curated genes, nine were found to be upregulated, three were downregulated, 7 produced insignificant expression, and data was unavailable for *GM36283*. The *USP18* gene was upregulated in high-fat diet-fed mice, with a significant influence over survival in LIHC patient. However, this gene was excluded since the gene expression profile was insignificant between the normal and primary tumor groups of LIHC patients. Upon searching for similar expression profiles, the two genes, *viz., RMND1* and *CYP3A16,* demonstrated identical gene expression in high-fat diet-fed mice treated with *Pi.* The *RMND1* coding for the required meiotic nuclear division 1 homolog *(S. cerevisiae)* protein was overexpressed in both datasets **(Fig. 5a)**. The LIHC patients showed a statistically significant difference

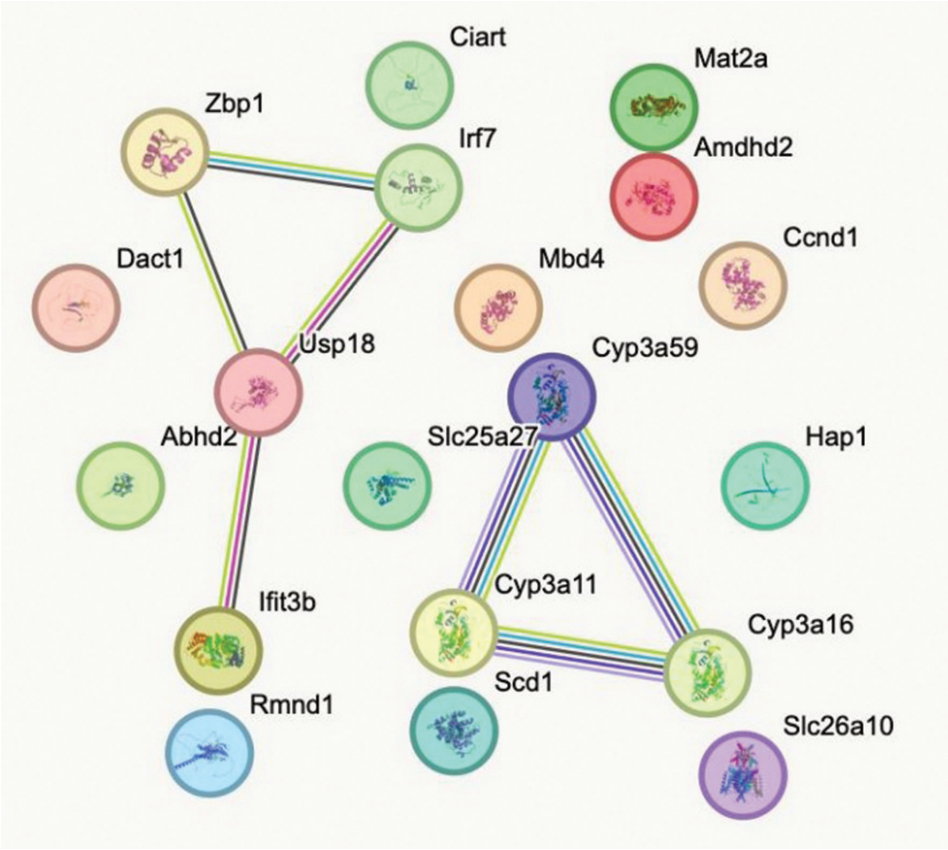

Figure 2. The protein-protein interaction network of the DEGs in *Mus musculus*.

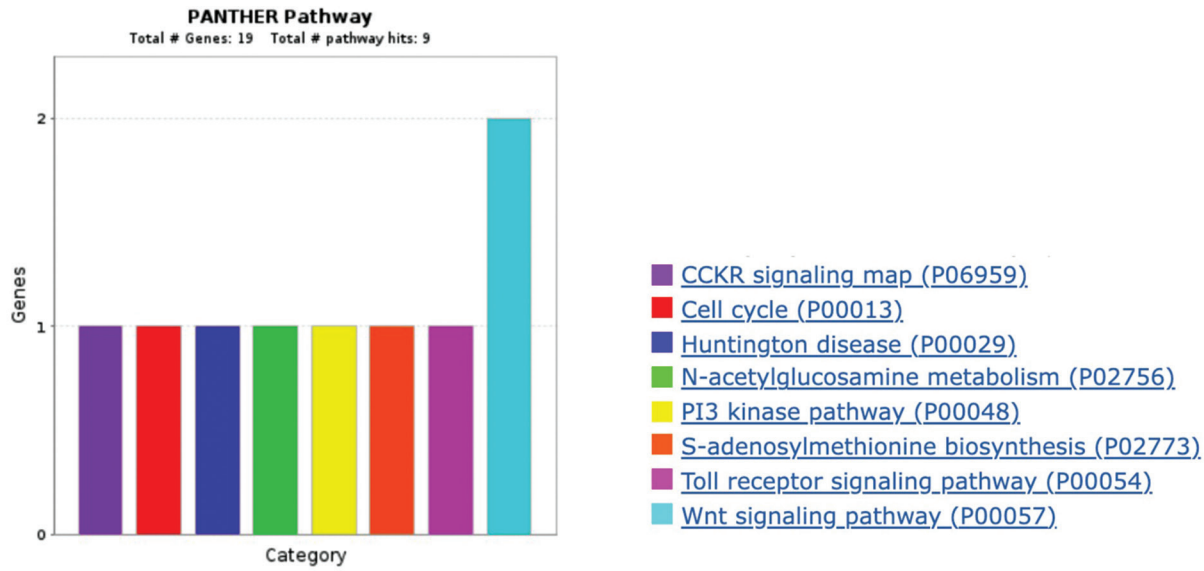

Figure 3. Gene ontology analysis demonstrating the pathways in which the DEGs are clustered in the *Mus musculus*.

in *RMND1* gene expression among the low and high-expression groups (p=1.55×10^{-11}) **(Fig. 5b)**. The other gene, *CYP3A59,* showed decreased expression in both datasets. The gene *CYP3A59* codes for cytochrome P450, family 3, subfamily a, polypeptide 59 **(Fig. 6a)**. The reduced expression of the mouse ortholog of *CYP3A59,* the *CYP3A43,* showed statistically significant downregulation in the LIHC patients (p=3.98×10^{-07}) **(Fig. 6b)**.

Kaplan-Meier survival analysis

The Kaplan-Meier survival plot predicted better survival outcomes in patients with low expression of *RMND1*. The hazard ratio (HR) was found to be 1.74 (95% CI-1.23 – 2.46), indicating that patients with increased expression of *RMND1* were 1.74 times at risk of death compared to the low expression group **(Fig. 5b)**. The divergence in surviv-

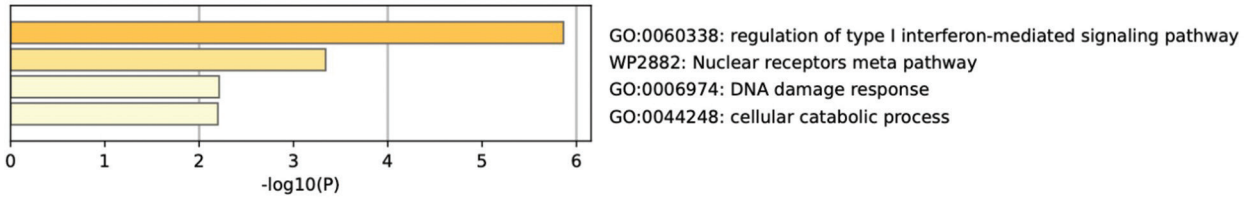

Figure 4. The graph demonstrates the gene enrichment pathways in which the DEGs are involved. The x-axis shows a gradient from 0-6, representing the log10 p values (data in bold represent high statistical significance).

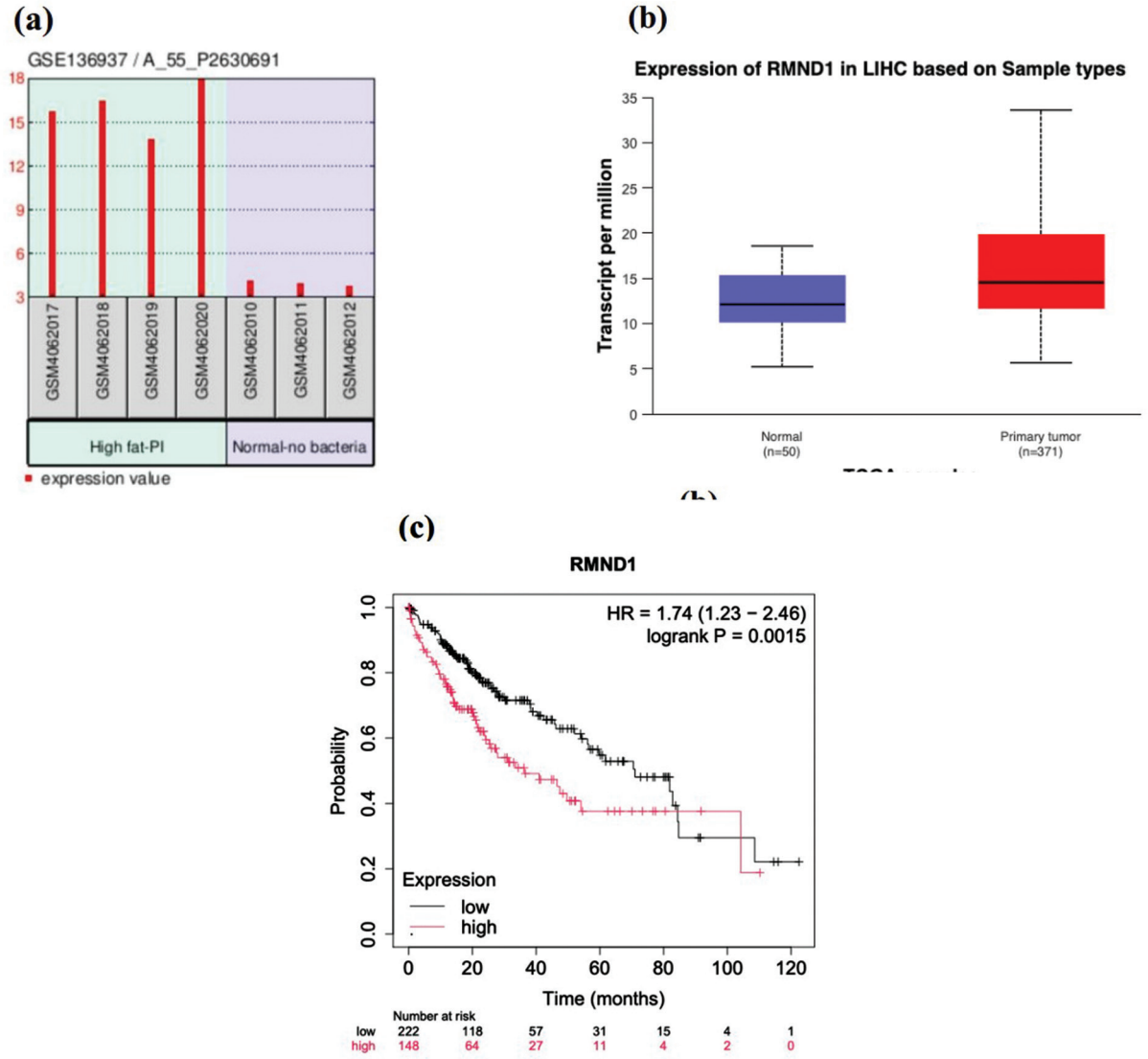

Figure 5. (**a**) Bar graph showing increased expression of *RMND1* gene in C57BL/6 mice treated with *Prevotella intermedia* (p=0.00436); (**b**) Box Whisker plot demonstrating the upregulation of *RMND1* gene in LIHC patients. A statistically significant increase in the level of *RMND1* was observed in the patients (p=1.55×10^{-11}); (**c**) Kaplan Meier survival analysis demonstrating poor prognosis in LIHC patients presenting with increased expression of *RMND1* gene (p=0.0015). A p-value of less than 0.05 was considered to be significant.

al probability starts early and becomes more pronounced between 20 - 30 months. Upon considering the five-year survival probability of LIHC patients, 31 patients survived among 222 individuals in the low-expression group, and 11 patients survived among 148 individuals in the high-expression group **(Fig. 5c)**. On the other hand, the Kaplan Meier survival plot indicated poor prognosis in patients with low expression of CYP2A43. The log-rank p-value suggests that the survival between the two groups was statistically significant (p=0.00018). The hazard ratio was found to be 0.51 (95% CI-0.36 – 0.73), indicating that the patients presenting with high expression of *CYP3A43* have

Folia Medica

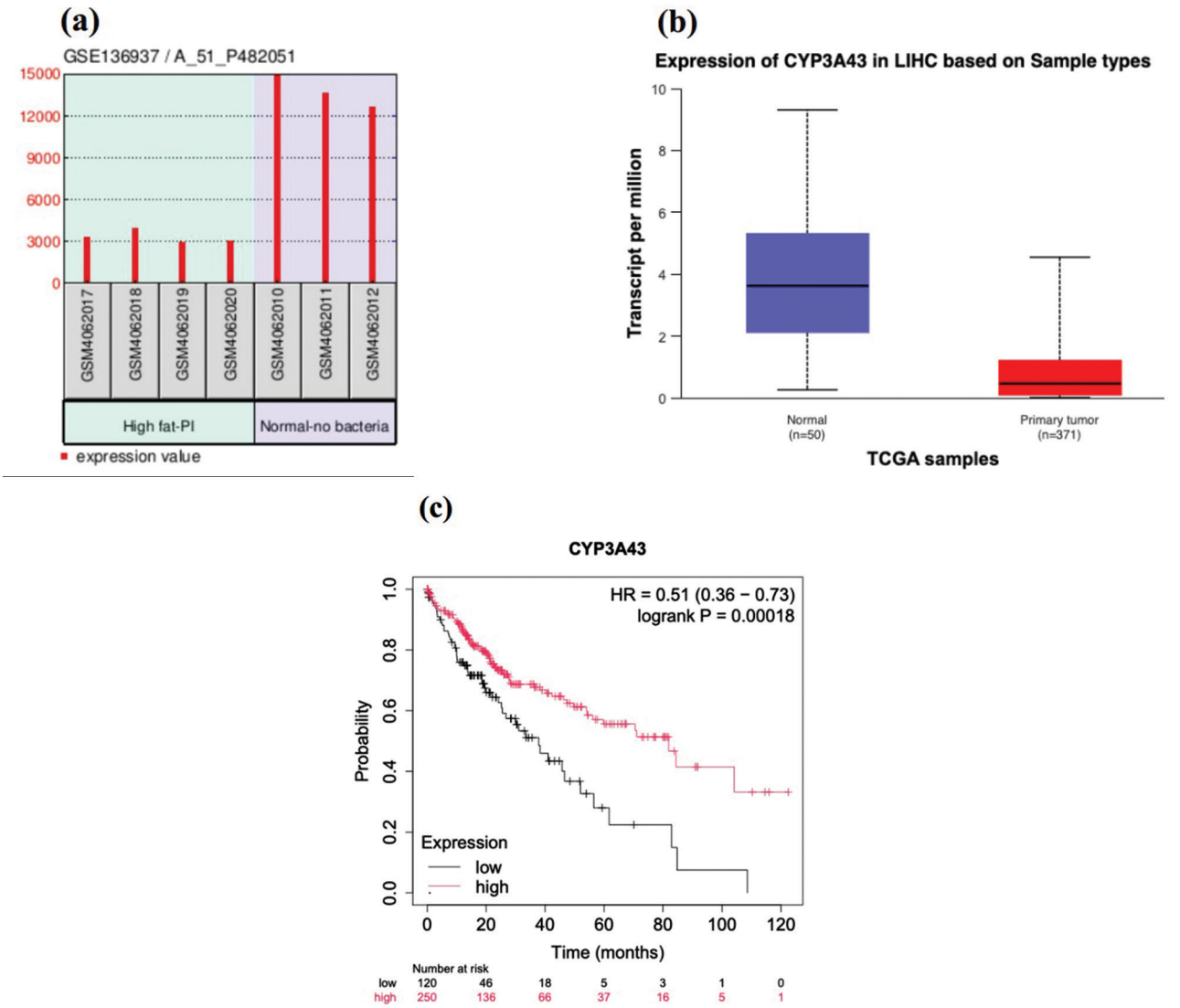

Figure 6. (**a**) Bar graph showing decreased expression of *CYP3A59* gene in C57BL/6 mice treated with *Prevotella intermedia* (p=0.00529); (**b**) Box Whisker plot demonstrating the downregulation of *CYP3A43* gene in LIHC patients. A statistically significant decrease in the level of *CYP3A43* was observed in the patients (p=3.98×10^{-07}); (**c**) Kaplan Meier survival analysis demonstrating poor prognosis in LIHC patients presenting with decreased expression of *CYP3A59/CYP3A43* gene (p=0.00018). A p-value of less than 0.05 was considered to be significant.

about half the risk of death when compared to the patients with low expression. Since the HR is less than 1, the increased expression of *CYP3A43* was associated with better survival. A 5-year survival analysis showed five individuals surviving among 120 patients in the low-expression group and 37 individuals surviving among 250 patients in the high-expression group.

Discussion

Metabolic disorders are a group of conditions that are characterized by dysregulation in the metabolic pathways. Mounting evidence has shown that metabolic disorders increase the risk of developing cancer.[20] Furthermore, the tumor microbiome is evolving as a newer dimension, leading to the initiation and supporting cancer progression. Targeting these oncomicrobiomes can be considered as an important strategy to revert the dysbiosis, thereby slowing down the progression of malignant transformation.[21] The oral cavity and gut microbiome are vital in maintaining cellular homeostasis, as they partly govern metabolism, immunomodulation, and signal transduction processes. Numerous studies have explored the role of oral and gastric microbiomes in health and disease. Dysbiosis observed in these microbial populations has often been associated with the progression of diseases such as diabetes mellitus, obesity, autoimmune disorders, cardiovascular and cerebrovascular diseases, and cancer. The association of *Porphyromonas endodontalis* with early-stage intramucosal esophageal squamous carcinoma and oral squamous cell carcinoma (OSCC)[22], *Fusobacterium nucleatum* with cancers of the

gastrointestinal tract[23], *Tannerella forsythia* and *Treponema denticola* with colon and bladder cancers[24], *Helicobacter pylori* with gastric and esophageal cancers[25] have been established through various experimental and clinical studies. Still, the underlying molecular mechanisms or the influence of co-morbid conditions on primary disease have not been unraveled yet. In this context, the present study was conducted to identify unique signatures established in the host in connection with co-morbid condition of obesity and infection with *Pi.* Interestingly, we could identify an extensive collection of upregulated and downregulated genes exclusively expressed in the experimental group of high-fat-fed mice exposed to *Pi* infection. The orthologous genes in LIHC patients showed a different expression profile; however, the two genes, *RMND1* and *CYP3A43*, exhibited similar expression patterns in both mice and humans. The differential expression observed in these two datasets positively correlated with the survival of the patients. The *RMND1* and *CYP3A43* genes revealed increased and decreased expression in LIHC patients, wherein the upregulation of the *RMND1* gene and downregulation in *CYP3A43* correlated with poor prognosis.

The *RMND1* gene, associated with mitochondrial function, has been implicated in cell proliferation and survival, which could explain its upregulation in HCC and its association with a poor prognosis. A study investigated breast cancer risk variants on chromosome 6q25, focusing on their associations with different breast cancer phenotypes and their regulation of critical genes, including *ESR1*, *RMND1*, and *CCDC170*. Using data from over 118,000 individuals, researchers identified five independent causal variants influencing estrogen receptor status, HER2 subtypes, mammographic density, and tumor grade. Functional analysis revealed that these variants modulate gene expression through enhancer and silencer elements, suggesting a complex regulatory landscape contributing to breast cancer susceptibility.[26] A study conducted by Woo et al. discussed the variants identified in the *RMND1* gene in association with chronic myeloid leukemia. Astonishingly, the expression of RMND1 expression was reduced in CML patients compared to healthy individuals. The A allele of the variant rs6931104 was found to significantly modulate the binding affinity of transcription factor RFX3, which decreased the expression of RMND1.[27] This observation was contrary to the results derived from the present study. Furthermore, the *RMND1* gene and its variants were found to show significant associations with different phenotypes, such as chronic kidney disease, dilated cardiomyopathy, and neurological involvement.[28] Many mitochondrial dysfunctions have been recently identified as related to *RMND1* gene variants.[29] Since mitochondrial defects are closely related to aging and cancer, it is worthwhile to investigate the genetic and epigenetic components encompassing the *RMND1* gene.

The downregulation of *CYP3A59/CYP3A43*, genes involved in drug metabolism and xenobiotic detoxification, may indicate a compromised ability to detoxify carcinogenic compounds, thereby facilitating carcinogenesis in the liver. Our findings align with previous research that has demonstrated the influence of periodontal pathogens on systemic inflammation and cancer progression.[30-32] The identification of *Pi* as a possible risk factor for liver cancer expands the understanding of how oral pathogens might contribute to extraoral malignancies. The systemic spread of periodontal bacteria or their inflammatory mediators could create a pro-tumorigenic environment in the liver, thereby contributing to the initiation and progression of HCC. The findings of our study contribute to the broader understanding of CYP3A enzyme involvement in disease, particularly about the downregulation of *CYP3A59/CYP3A43* in the context of *Pi*-induced LIHC.

A study highlighted the essential role of mouse CYP enzymes and their human orthologs in metabolizing both endogenous and exogenous compounds. It highlights the impact of CYP enzyme activity on metabolic and toxicological processes, which aligns with our observations in liver cancer progression.[33] A study by Klyushova and team emphasized the broad substrate specificity of the *CYP3A* subfamily, including *CYP3A43*, and its critical role in maintaining physiological balance while also being implicated in various pathologies; this aligns with our finding that *CYP3A59/CYP3A43* downregulation could contribute to a disrupted metabolic environment conducive to carcinogenesis.[34] Another study explored the role of *CYP3A4* in vitamin D metabolism and its interactions with various factors, highlighting how genetic polymorphisms and environmental influences can alter enzyme activity. This concept parallels our observation of how *Pi* infection may modulate *CYP3A59/CYP3A43* expression, potentially impacting liver cancer outcomes.[35] Together, these studies reinforce the significance of CYP3A enzymes in disease development and provide context for our findings on the role of *CYP3A59/CYP3A43* in HCC.

While our study provides important insights into the potential role of *CYP3A59/CYP3A43* and other genes in the progression of hepatocellular carcinoma in the context of *Pi* infection, it is crucial to acknowledge that these findings are based on in-silico analysis, which could be a major limitation of the study. However, the preliminary results obtained from our study can serve as the initiation point for conducting further research involving clinical studies on microbial dysbiosis as a key component of tumorigenesis in patients with severe metabolic disorders. Other limitations of the study were (**a**) the microbial exposure factors of the patients of the study is not well established, (**b**) epigenetic and epitranscriptomic factors also play a key role in the modulation of gene expression, hence it is noteworthy to investigate these mechanisms to acquire a more vivid picture on the molecular mechanisms, (**c**) dietary habits and underlying co-morbid conditions can affect the microbial load, thereby elevating or diminishing the risk of malignant transformations, therefore it is vital to accurately identify the microbial pathogens and quantify them to derive strong association with the cancer type.

Until such studies are conducted, the connections drawn from our research remain hypothetical and should be viewed as a foundation for future exploration rather than definitive conclusions.

Conclusion

This study explored the potential link between metabolic disorders, *Pi* infection, and hepatocellular carcinoma progression by identifying differentially expressed genes, particularly *CYP3A59/CYP3A43* and *RMND1*. Our findings suggest that these genes could play a significant role in the pathogenesis of HCC, possibly through their involvement in metabolic and inflammatory pathways. However, as this research is based on in-silico analysis, further clinical investigations are necessary to confirm these associations and fully understand the biological mechanisms at play. This study serves as a preliminary step towards uncovering the complex interactions between oral pathogens and liver cancer, highlighting the need for more comprehensive studies to establish *Prevotella intermedi*'s role in HCC and explore potential therapeutic targets.

Conflict of interest

The authors declare that there is no conflict of interest in this study.

Funding

None

Acknowledgements

The authors are grateful to all the consorts and groups involved in the compilation of data from patients for public use. Our sincere thanks also go to all the patients who have indirectly contributed to the scientific community by providing consent for sharing their data for research use.

References

1. Toh MR, Wong EYT, Wong SH, et al. Global epidemiology and genetics of hepatocellular carcinoma. Gastroenterology 2023; 164(5):766–82. doi: 10.1053/j.gastro.2023.01.033
2. Shree Harini K, Ezhilarasan D. Wnt/beta-catenin signaling and its modulators in nonalcoholic fatty liver diseases. Hepatobiliary Pancreat Dis Int 2023; 22(4):333–45. doi: 10.1016/j.hbpd.2022.10.003
3. Liu B, Zhou Z, Jin Y, et al. Hepatic stellate cell activation and senescence induced by intrahepatic microbiota disturbances drive progression of liver cirrhosis toward hepatocellular carcinoma. J Immunother Cancer 2022; 10(1):e003069. doi: 10.1136/jitc-2021-003069
4. Ezhilarasan D, Najimi M. Deciphering the possible reciprocal loop between hepatic stellate cells and cancer cells in the tumor microenvironment of the liver. Crit Rev Oncol Hematol 2023; 182:103902. doi: 10.1016/j.critrevonc.2022.103902
5. Akil A, Endsley M, Shanmugam S, et al. Fibrogenic gene expression in hepatic stellate cells induced by HCV and HIV replication in a three cell co-culture model system. Sci Rep 2019; 9(1):568. doi: 10.1038/s41598-018-37071-y
6. You H, Wang X, Ma L, et al. Insights into the impact of hepatitis B virus on hepatic stellate cell activation. Cell Commun Signal 2023; 21(1):70. doi: 10.1186/s12964-023-01091-7
7. Dakshinya M, Anitha P, Girija AS, et al. Differential gene expression profile in *Porphyromonas gingivalis* treated human gingival keratinocytes and their role in the development of HNSCC. J Oral Biol Craniofac Res 2025; 15(1):48–56. doi: 10.1016/j.jobcr.2024.11.007
8. Yamazaki K, Kato T, Tsuboi Y, et al. Oral pathobiont-induced changes in gut microbiota aggravate the pathology of nonalcoholic fatty liver disease in mice. Front Immunol 2021; 12:766170. doi: 10.3389/fimmu.2021.766170
9. Zhang S, Zhao Y, Lalsiamthara J, et al. Current research progress on Prevotella intermedia and associated diseases. Crit Rev Microbiol 2024; 1-8. doi: 10.1080/1040841X.2024.2390594
10. Qin Y, Li Z, Liu T, et al. *Prevotella intermedia* boosts OSCC progression through ISG15 upregulation: a new target for intervention. J Cancer Res Clin Oncol 2024; 150(4):206. doi: 10.1007/s00432-024-05730-5
11. Deepika BA, Ramamurthy J, Kannan B, et al. Overexpression of insulin-like growth factor-2 mRNA-binding protein 1 is associated with periodontal disease. J Oral Biol Craniofac Res 2024; 14(5):494–9. doi: 10.1016/j.jobcr.2024.06.001
12. Szklarczyk D, Gable AL, Lyon D, et al. STRING v11: protein-protein association networks with increased coverage, supporting functional discovery in genome-wide experimental datasets. Nucleic Acids Res 2019; 47(D1):D607–D613. doi: 10.1093/nar/gky1131
13. Mi H, Thomas P. PANTHER pathway: an ontology-based pathway database coupled with data analysis tools. Methods Mol Biol 2009; 563:123–40. doi: 10.1007/978-1-60761-175-2_7
14. Mi H, Ebert D, Muruganujan A, et al. PANTHER version 16: a revised family classification, tree-based classification tool, enhancer regions and extensive API. Nucleic Acids Res 2021; 49(D1):D394–D403. doi: 10.1093/nar/gkaa1106
15. Zhou Y, Zhou B, Pache L, et al. Metascape provides a biologist-oriented resource for the analysis of systems-level datasets. Nat Commun 2019; 10(1):1523. doi: 10.1038/s41467-019-09234-6
16. Chandrashekar DS, Karthikeyan SK, Korla PK, et al. UALCAN: An update to the integrated cancer data analysis platform. Neoplasia 2022; 25:18–27. doi: 10.1016/j.neo.2022.01.001
17. Győrffy B. Integrated analysis of public datasets for the discovery and validation of survival-associated genes in solid tumors. Innovation (Camb) 2024; 5(3):100625. doi: 10.1016/j.xinn.2024.100625
18. Barrett T, Wilhite SE, Ledoux P, et al. NCBI GEO: archive for functional genomics data sets--update. Nucleic Acids Res 2013; 41(Database issue):D991–5. doi: 10.1093/nar/gks1193
19. Chandrashekar DS, Bashel B, Balasubramanya SAH, et al. UALCAN: A portal for facilitating tumor subgroup gene expression and survival analyses. Neoplasia 2017; 19(8):649–58. doi: 10.1016/j.neo.2017.05.002
20. Taranto D, Kloosterman DJ, Akkari L. Macrophages and T cells

in metabolic disorder-associated cancers. Nat Rev Cancer 2024; 24(11):744–67. doi: 10.1038/s41568-024-00743-1
21. Zhou X, Kandalai S, Hossain F, et al. Tumor microbiome metabolism: A game changer in cancer development and therapy. Front Oncol 2022; 12:933407. doi: 10.3389/fonc.2022.933407
22. Chen H, Jiang X, Zhu F, et al. Characteristics of the oral and gastric microbiome in patients with early-stage intramucosal esophageal squamous cell carcinoma. BMC Microbiol 2024; 24(1):88. doi: 10.1186/s12866-024-03233-4
23. Selvaraj A, McManus G, Healy CM, et al. *Fusobacterium nucleatum* induces invasive growth and angiogenic responses in malignant oral keratinocytes that are cell line- and bacterial strain-specific. Front Cell Infect Microbiol 2024; 14:1417946. doi: 10.3389/fcimb.2024.1417946
24. Lund Håheim L, Thelle DS, Rønningen KS, et al. Low level of antibodies to the oral bacterium *Tannerella forsythia* predicts bladder cancers and *Treponema denticola* predicts colon and bladder cancers: A prospective cohort study. PLoS One 2022; 17(8):e0272148. doi: 10.1371/journal.pone.0272148
25. Yan X, Zeng H, Li H, et al. The current infection with *Helicobacter pylori* and association with upper gastrointestinal lesions and risk of upper gastrointestinal cancer: Insights from multicenter population-based cohort study. Int J Cancer 2024; 155(7):1203–11. doi: 10.1002/ijc.34998
26. Dunning AM, Michailidou K, Kuchenbaecker KB, et al. Breast cancer risk variants at 6q25 display different phenotype associations and regulate ESR1, RMND1 and CCDC170. Nat Genet 2016; 48(4):374–86. doi: 10.1038/ng.3521
27. Woo YM, Kim S, Park JH, et al. Evidence that 6q25.1 variant rs6931104 confers susceptibility to chronic myeloid leukemia through RMND1 regulation. PLoS One 2019; 14(6):e0218968. doi: 10.1371/journal.pone.0218968
28. Gupta A, Colmenero I, Ragge NK, et al. Compound heterozygous RMND1 gene variants associated with chronic kidney disease, dilated cardiomyopathy and neurological involvement: a case report. BMC Res Notes 2016; 9:325. doi: 10.1186/s13104-016-2131-2
29. Garcia-Diaz B, Barros MH, Sanna-Cherchi S, et al. Infantile encephaloneuromyopathy and defective mitochondrial translation are due to a homozygous RMND1 mutation. Am J Hum Genet 2012; 91(4):729–36. doi: 10.1016/j.ajhg.2012.08.019
30. Liu J, Zhou L, Sun L, et al. Association between intestinal *Prevotella copri* abundance and glycemic fluctuation in patients with brittle diabetes. Diabetes Metab Syndr Obes 2023; 16:1613–21. doi: 10.2147/DMSO.S412872
31. Lopes MP, Cruz ÁA, Xavier MT, et al. *Prevotella intermedia* and periodontitis are associated with severe asthma. J Periodontol 2020; 91(1):46–54. doi: 10.1002/JPER.19-0065
32. Lo CH, Wu DC, Jao SW, et al. Enrichment of *Prevotella intermedia* in human colorectal cancer and its additive effects with *Fusobacterium nucleatum* on the malignant transformation of colorectal adenomas. J Biomed Sci 2022; 29(1):88. doi: 10.1186/s12929-022-00869-0
33. Hrycay EG, Bandiera SM. Expression, function and regulation of mouse cytochrome P450 enzymes: comparison with human P450 enzymes. Curr Drug Metab 2009; 10(10):1151–83. doi: 10.2174/138920009790820138
34. Klyushova LS, Perepechaeva ML, Grishanova AY. The role of CYP3A in health and disease. Biomedicines 2022; 10(11):2686. doi: 10.3390/biomedicines10112686
35. Kasarla SS, Garikapati V, Kumar Y, et al. Interplay of vitamin D and CYP3A4 polymorphisms in endocrine disorders and cancer. Endocrinol Metab (Seoul) 2022; 37(3):392–407. doi: 10.3803/EnM.2021.1349